

DSS 13 Phase II Pedestal Room Microwave Layout

T. Cwik and J. C. Chen
Ground Antennas and Facilities Engineering Section

This article describes the design and predicted performance of the microwave layout for three-band operation of the beam waveguide antenna DSS 13. Three pedestal-room microwave candidate layout designs were produced for simultaneous X-/S- and X-/Ka-band operation. One of the three designs was chosen based on given constraints, and for this design the microwave performance was estimated.

I. Introduction

This article describes the design and predicted performance of the microwave layout for three-band operation of the beam waveguide (BWG) antenna DSS 13 [1].¹ This design is part of the Phase II implementation of the antenna. The relevant microwave system is shown in Fig. 1 for a single feed in the pedestal room. The object of this work was to create pedestal-room microwave layouts for simultaneous X-/S- and X-/Ka-band operation. The center-band frequencies S-band (2.295 GHz), X-band (8.450 GHz), and Ka-band (32.000 GHz) were used in this design. Because the antenna had already been constructed, the obvious constraints of pedestal room size, BWG geometry, etc. were in place for this work. The size and shape of all BWG mirrors, including the basement ellipse, were set, although this mirror will be allowed to rotate to view different feed systems.

¹M. Britcliff, ed., *DSS-13 Beam Waveguide Antenna Project: Phase I Final Report*, JPL D-8451 (internal document), Jet Propulsion Laboratory, Pasadena, California, May 15, 1991.

II. Candidate Designs

Based on the above constraints, three candidate designs for the pedestal room were generated. The final design will take up some sector of the pedestal room floor, allowing for the possibility of the S-/X- and X-/Ka-band systems' having different optical paths, switched by the rotating ellipsoidal mirror. The defining constraint which emerged from the generation of these designs was the minimization of the area containing the apertures in the X-/Ka-band dichroic plate. (The dichroic plate has an inner aperture filled area along with an outer solid skirt.) This constraint will be examined in more detail in Section III.

A. Single-Sided, Vertical S-Band Design

The first design considered placed the S-, X-, and Ka-band horns vertically along one side of the ellipsoidal mirror (Fig. 2). S-/X- and X-/Ka-band dichroic plates and a Ka-band flat plate reflect the specific bands to the phase centers at f_3 . The S-/X-band dichroic plate will be removed for X-/Ka-band operation since it is not designed

to pass the Ka-band. Vertical placement of the three horns preserves a single-plane 60-deg optical geometry. The immediate drawback of this design is the lack of room for a conventional S-band horn to be physically located in the existing pedestal room (Fig. 2 inset). The horn itself, without associated subsystems, extends approximately 66 in. below the existing pedestal room floor. Profiled S-band horns, which reduce the horn length, were also considered, but these did not eliminate the need for excavation of the pedestal room.

B. Single-Sided, Horizontal S-Band Horn Design

To eliminate the need to excavate the pedestal room, the second design places the S-band horn horizontally, as shown in Fig. 3(a). To preserve the correct electromagnetic optical design, the S-band horn and S-/X-band dichroic plate are both rotated in two planes. After considering the horn and plate to be fixed together, the proper orientation results from a 90-deg rotation up from the vertical to horizontal planes, and a rotation in the horizontal plane by 35.3 deg toward the ellipsoidal mirror. The S-band horn is now lying in the x-y plane at an angle such that rays from the horn reflect off the dichroic plate and down at a 60-deg angle to the ellipsoidal mirror. The plan view of this layout is shown in Fig. 3(b).

C. Double-Sided, Horizontal S-Band Design

The third candidate design is motivated by the close fit between feed systems and dichroic plates in the previous design. Depending on the feed support and associated amplifier and microwave subsystem, more space than shown is needed around the three feedhorns. For example, for an ultra-low noise amplifier Ka-band system, the dewar surrounding the Ka-band horn may extend 9 to 15 in. out from the center of the Ka-band horn, physically interfering with the X-/Ka-band dichroic plate. To gain more space, the double-sided design was produced, as shown in Fig. 4(a). The X-band feed system is duplicated, and the S-/X-band system is positioned along an optical path different from the X-/Ka-band system. This design relaxes the tight fit between feed systems and dichroic plates. The plan view of this arrangement is shown in Fig. 4(b). The 45-deg angle between the X-/S- and X-/Ka-band optical paths is chosen to allow clearance between the systems and to minimize the floor area used.

D. Computer-Aided Design of Candidate Designs

Because of the three-dimensional geometry, as well as the close fit between components in the designs, a computer-aided design (CAD) system was used to draft each of the three candidates. The ellipsoidal mirror was

drawn into the pedestal room, and the various components added. Estimated thicknesses of the flat and dichroic plates were included as well as the backing of the ellipsoidal mirror. Feedhorn mounting fixtures and the envelopes of anticipated microwave subassemblies were similarly added and color-coded by frequency band. The three candidate designs were drawn separately and optic rays were added to define the optical envelope of the layout. The CAD system can continuously rotate and zoom the image on the screen, allowing visualization of the design from different viewing angles and distances, and has the capability of measuring distances among components. To provide a hard copy of this visualization, a video recorder was used to create an 8-min video of the three designs as the images were rotated and zoomed.² This video is available from the authors for viewing.

III. X-/Ka-Band Dichroic Plate Constraint

The dichroic plates needed in the above layouts are for simultaneous Ka-band (pass band) and X-band (reflecting band), and X-band (pass band) and S-band (reflecting band) operations. It was found that the X-/Ka-band plate was a defining constraint of the layout.

The location and the size of the dichroic plates in the layouts are dependent on the spillover loss, mechanical layout, cost, and the constraints of fabrication. The dichroic plates need to meet three criteria: (1) The size is electromagnetically big enough to minimize the spillover loss—the bigger the dichroic plate, the lower the spillover loss at a given location. (2) The closer the plate is to the focal point of the ellipsoidal mirror, the smaller the spillover loss is for a given-size plate. Hence, the dichroic plate is placed as close to the focal point of the ellipsoid as possible to reduce the plate size and minimize spillover loss, but to give enough clearance to other components in the mechanical layout. (3) The cost of the dichroic plate is roughly proportional to the number of holes on the plate. Therefore, the size of the dichroic plate has to remain within the budget and under a 38-in. diameter, which is the maximum size that can be fabricated.

The layout for the X-/Ka-band system is shown in Fig. 4(a). The X-/Ka-band dichroic plate is a 28-in.-diameter round plate with approximately 12,000 holes and is 28 in. away from the focal point of the ellipsoidal mirror in the pedestal room. The mechanical layout shows no

² T. Cwik, J. Chen, and G. Hale, "DSS 13 Phase II Microwave Layout Designs," videotape, Ground Antennas and Facilities Engineering Section, Jet Propulsion Laboratory, Pasadena, California, August 1990.

blockage and clearance to all nearby components, giving the minimum size for the X-/Ka-band plate.

IV. Design Choice

Based on the above constraints and layouts, the third candidate was chosen for implementation. The first candidate was ruled out because of the need for excavating the pedestal room. Of the second and third candidates, the third was chosen because of maximum room among components. If floor space becomes a premium, the components can be rearranged into the second design, allowing for future systems to be implemented.

V. Predicted Performance

The gain of the antenna for the chosen design layout was estimated by physical optics (PO) integration of currents induced on the mirrors. The breakdown of gain and spillover losses in the beam waveguide and a benchmark calculation at f_1 are shown in Fig. 5 for the three bands. The estimate for a given frequency is found from a succession of PO integrations, beginning with a calculation of the fields reflected from the ellipse due to a feed pattern at f_3 . This field distribution is the input pattern used in a PO-PO integration through the two parabolas P_1 and P_2 . Flat mirrors F_1 and F_2 are neglected in this calculation.

The field distribution emerging from P_1 is then the input to a PO/Jacobi-Bessel calculation for the field radiated from the sub-/main reflector system. The listed gain at f_3 is the result of this series of calculations. Spillover estimates past the BWG mirrors are also listed in Fig. 5. Spillover past the basement mirrors (B) is the amount of energy spilling past the mirrors in the electromagnetic path at the given frequency. For example, at the X-/Ka-band side, the Ka-band feed distribution sees the Ka-band flat plate and X-/Ka-band dichroic plate, while the X-band field distribution sees only the X-/Ka-band dichroic plate. Spillover past the flat plates F_1 and F_2 was estimated indirectly from a separate calculation, rather than from the

succession of PO calculations. For a benchmark estimate, the antenna gain due to a 29-dBi horn pattern referenced at f_1 is included.

Extra analysis was extended to the S-band system because of the loss of gain relative to a theoretical feed pattern at f_1 . The central conclusion drawn was that the S-band field defocuses as it propagates through the BWG. That is, for a 22.4-dBi S-band horn referenced to f_3 , the resulting field propagated through the BWG and referenced to f_1 is not a 29-dBi amplitude field with corresponding phase distribution that properly illuminates the sub-/main reflector system, producing maximum gain. The defocusing mainly results as the feed pattern is magnified by the ellipsoidal basement mirror. Ideally, the 22.4-dBi feed pattern at f_3 should refocus into a 29-dBi pattern referenced to f_2 . This field would then propagate through the next BWG section to properly refocus at f_1 with no change of gain. It was found that the S-band field refocuses approximately 90 in. above the f_2 focus, improperly illuminating the next section of the BWG.

Numerical experiments were made to move the focus back toward f_2 . A method was developed which partially accomplished this by defocusing the horn at f_3 , while changing its gain. For example, by defocusing the horn away from the S-/X-band dichroic plate and increasing the horn gain, the resultant focus could be pulled back toward f_2 . Although this technique could modify the horn focus relative to f_2 , the change in overall antenna gain was not significant enough to add the defocusing to the design. The conclusion drawn from the S-band study was that the ellipsoidal mirror, being approximately 20 wavelengths at S-band, is simply not large enough to focus the field near f_2 and therefore properly illuminate the next section of the BWG.

VI. Epilogue

Implementation of this design began in the first quarter of 1991. Further Ka-band design work is being considered due to dichroic plate cost and size of the ultra-low noise amplifier and associated dewar.

Acknowledgment

The authors gratefully acknowledge the skilled assistance of Gary Hale of the Prototype and Mechanical Fabrication Services Section, for the CAD of the above layouts.

Reference

- [1] T. Veruttipong, W. Imbriale, and D. Bathker, "Design and Performance Analysis of the DSS-13 Beam Waveguide Antenna," *TDA Progress Report 42-101*, vol. January–March 1990, Jet Propulsion Laboratory, Pasadena, California, pp. 99–113, May 15, 1990.

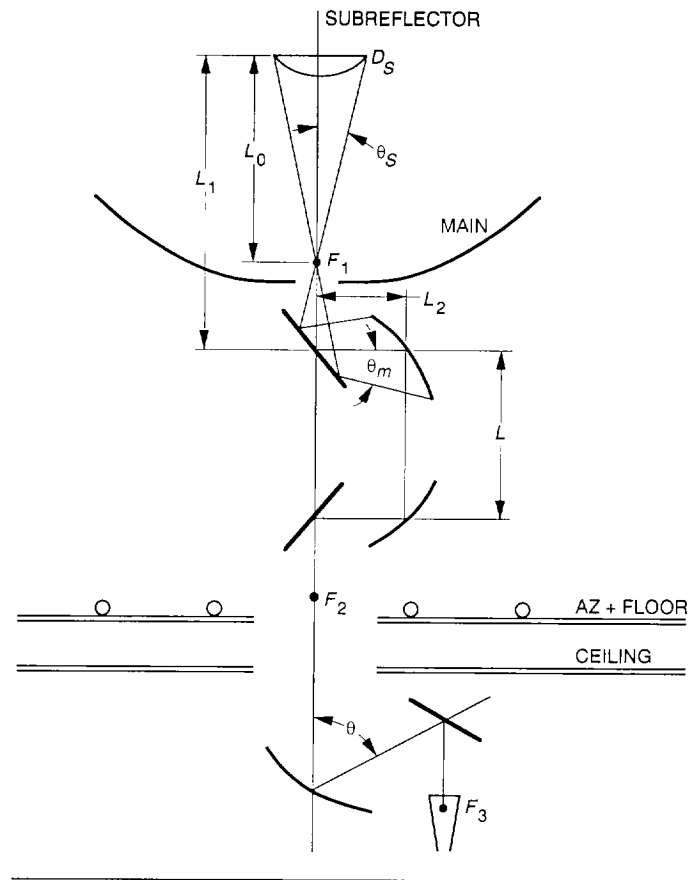


Fig. 1. Beam waveguide optics of DSS 13.

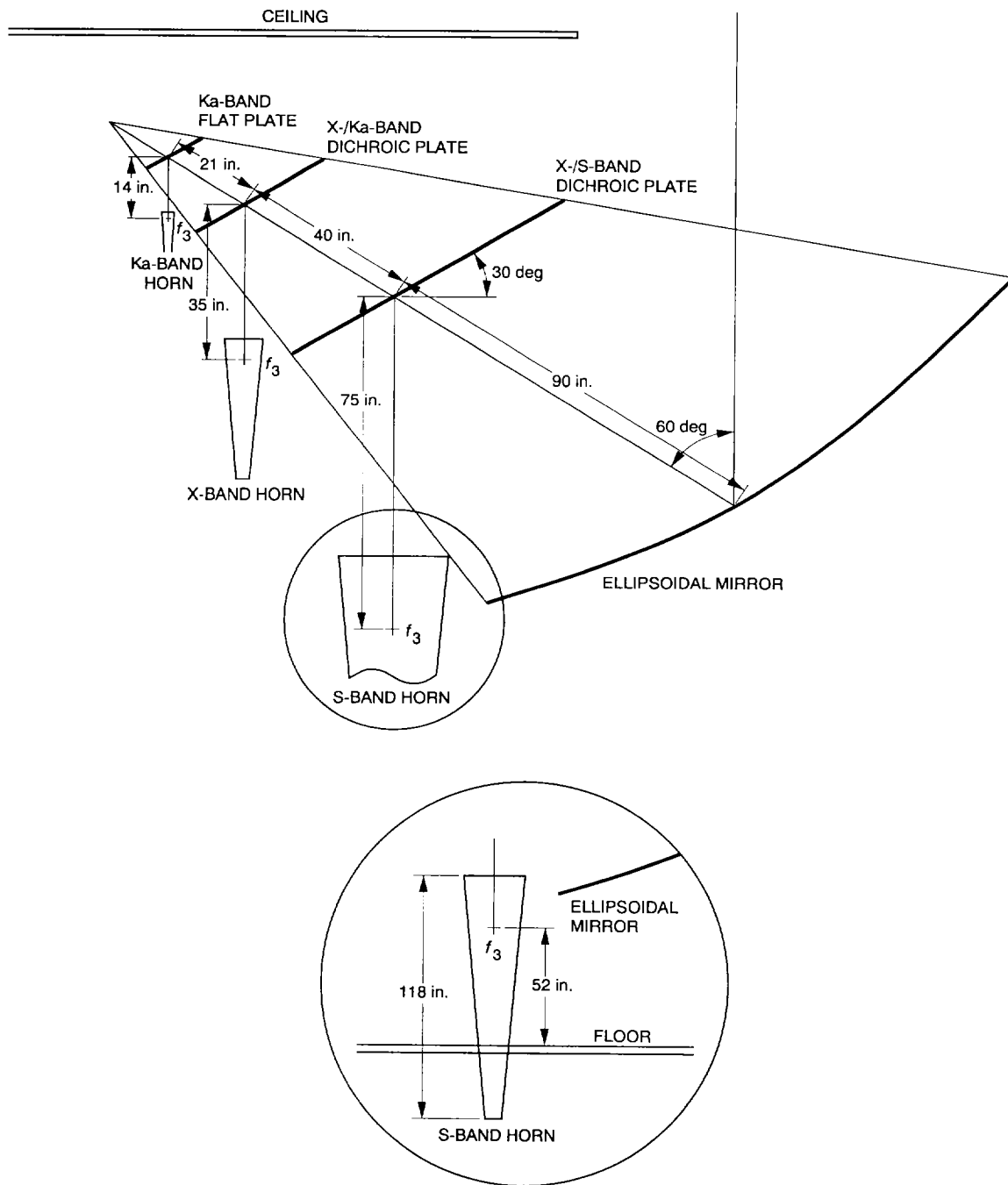


Fig. 2. Pedestal room optics for single-sided, vertical S-band horn design. Inset shows detail of vertical S-band horn with existing floor.

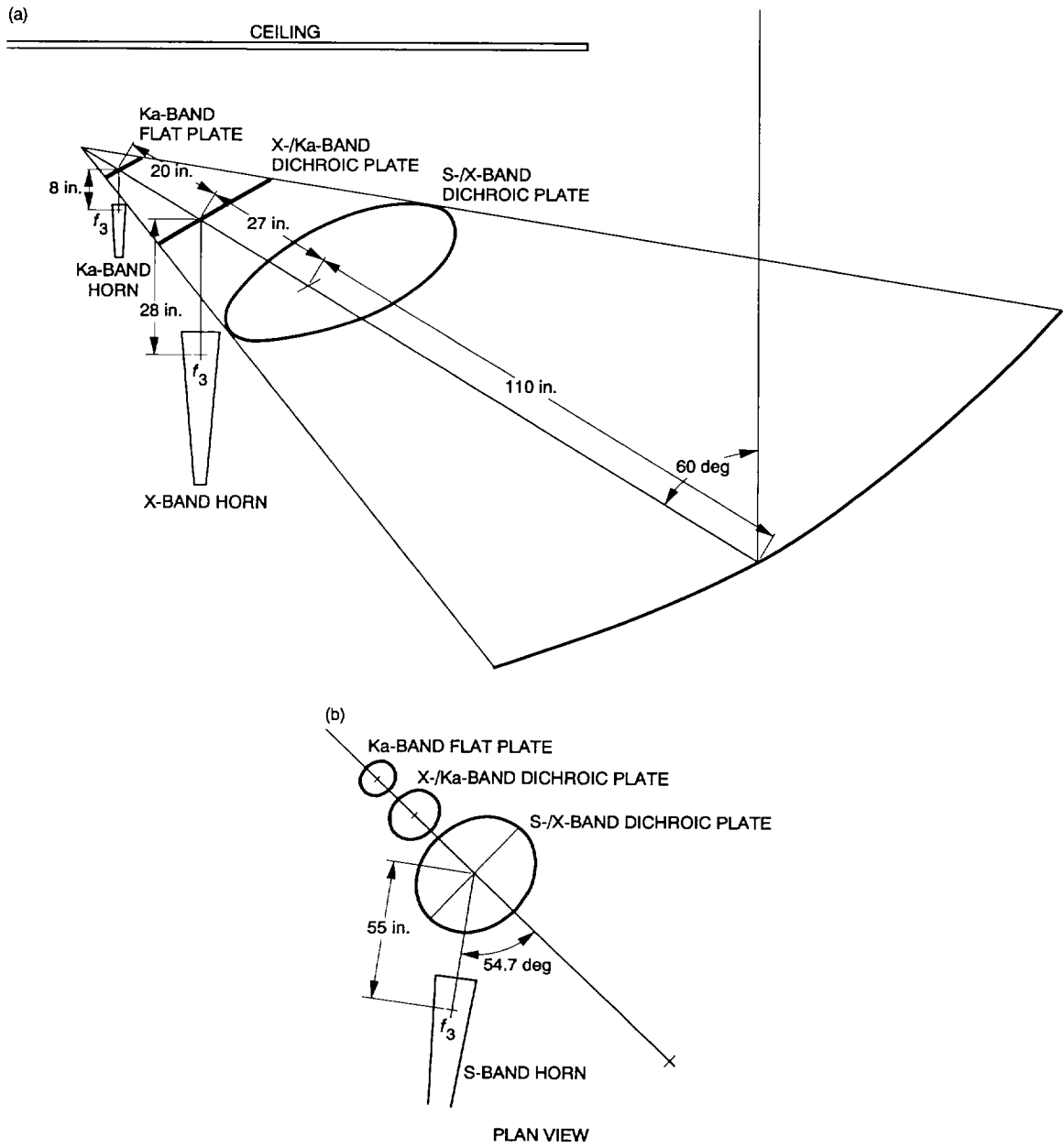


Fig. 3. Single-sided horizontal S-band horn geometry: (a) pedestal room optics and (b) plan view.

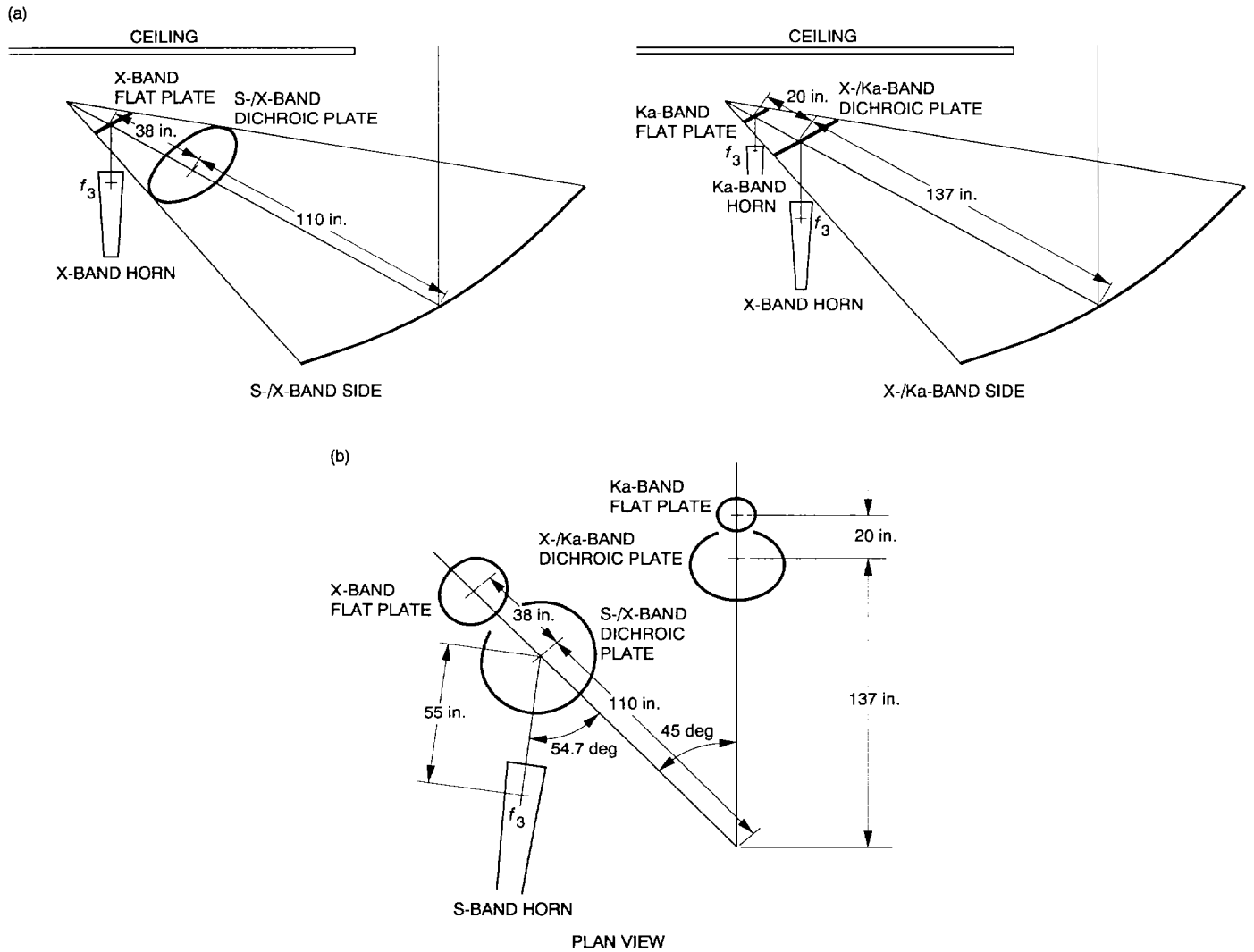
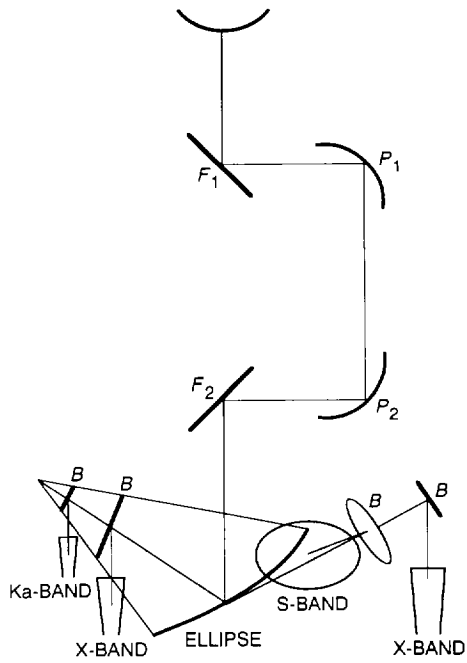


Fig. 4. Double-sided horizontal S-band horn geometry: (a) S-/X- and X-/Ka-band and (b) plan view with 45-deg offset angle.



BAND	BWG SPILLOVER, dBi					GAIN ^a , dBi f_3	GAIN ^b , dBi f_1
	ΣB	ELLIPSE	$P_1 + P_2$	$F_1 + F_2$	TOTAL		
S	0.01	0.08	0.55	0.14	0.78	55.85	57.47
X	0.03	0.07	0.06	0.02	0.17	69.00	69.20
Ka	0.03	0.06	0.05	0.01	0.14	80.54	80.70

^a DOES NOT INCLUDE RMS, DICHOIC, WAVEGUIDE, etc. LOSSES.

^b 29-dBi HORN PATTERN REFERENCED AT f_1 .

Fig. 5. Beam waveguide geometry and predicted performance for double-sided design.